Suppression of superconductivity in $Lu_xZr_{1-x}B_{12}$: Evidence of static magnetic moments induced by nonmagnetic impurities

N. E. Sluchanko,[1,2,*] A. N. Azarevich,[1] M. A. Anisimov,[1] A. V. Bogach,[1] S. Yu. Gavrilkin,[3] M. I. Gilmanov,[2] V. V. Glushkov,[1,2] S. V. Demishev,[1,2] A. L. Khoroshilov,[2] A. V. Dukhnenko,[4] K. V. Mitsen,[3] N. Yu. Shitsevalova,[4] V. B. Filippov,[4] V. V. Voronov,[1] and K. Flachbart[5]

[1]*A. M. Prokhorov General Physics Institute of RAS, 38 Vavilov Street, 119991 Moscow, Russia*

[2]*Moscow Institute of Physics and Technology, 9 Institutskiy Lane, 141700 Dolgoprudny, Moscow Region, Russia*

[3]*P. N. Lebedev Physical Institute of RAS, 53 Leninskiy Avenue, 119991 Moscow, Russia*

[4]*Institute for Problems of Materials Science of National Academy of Sciences of Ukraine, 3 Krzhizhanovskogo Street, 03680 Kiev, Ukraine*

[5]*Institute of Experimental Physics of SAS, 47 Watsonova Street, SK-04001 Košice, Slovak Republic*

(Received 30 July 2015; published 23 February 2016)

Based on low-temperature resistivity, heat capacity, and magnetization investigations, we show that the unusually strong suppression of superconductivity in $Lu_xZr_{1-x}B_{12}$ ($x < 8\%$) BCS-type superconductors is caused by the emergence of static spin polarization in the vicinity of nonmagnetic lutetium impurities. The analysis of the obtained results points to a formation of static magnetic moments with $\mu_{\rm eff} \approx 6\mu_B$ per Lu^{3+} ion ($^1S_0$ ground state, $4f^{14}$ configuration) incorporated in the superconducting ZrB_{12} matrix. The size of these spin-polarized nanodomains was estimated to be about 5 Å.

DOI: 10.1103/PhysRevB.93.085130

I. INTRODUCTION

The discovery of superconductivity at $T_c \approx 39$ K in MgB_2 [1] has stimulated a significant interest into the studies of a wide class of the alkaline-earth, rare-earth, and transition-metal borides. Among them, in the family of higher borides RB_{12}, zirconium dodecaboride (ZrB_{12}) is a BCS superconductor with the highest $T_c \approx 6$ K [2,3]. An intriguing detail found in ZrB_{12} is the formation of Cooper pairs through quasilocal vibrations involving Zr^{4+} ions located within truncated B_{24} octahedrons in the UB_{12}-type fcc crystal structure [2–5]. In studies of the Einstein phonon mediated superconductivity in ZrB_{12}, the authors of Refs. [2–9] argue that s-wave pairing is characteristic for this compound, and that in this case the Ginzburg-Landau parameter κ is located in the nearest vicinity to the threshold value $\kappa_c = 2^{-1/2}$. Moreover, a crossover from type-I to type-II/1 [10] superconductivity with decreasing temperature was deduced in Ref. [3] from heat capacity and magnetization measurements. On the other hand, in Ref. [11] the superconductivity in ZrB_{12} was interpreted in terms of d-wave pairing and a two-gap type-II regime was identified with the parameters $\kappa_p = 3.8$ and $\kappa_d = 5.8$. Additionally, a large size pseudogap ($\Delta \sim 7.3$ meV) has been detected by employing high resolution photoemission spectroscopy in ZrB_{12} above T_c, and the proximity to the quantum fluctuation regime was predicted from *ab initio* band structure calculations [12]. Certain similarities with cuprate high-temperature superconductors (HTSC) may be also supposed to revive interest in studies of this low-temperature superconductor.

In the case of nonmagnetic impurity substitutions and their impact on superconducting properties, one can choose between various scenarios, because the pair-breaking mechanism for these defects in various models differs. According to Anderson's theorem [13,14] and its extension to non-s-wave superconductivity (see, e.g., Refs. [15,16]), it is expected that already a small amount of nonmagnetic impurities can dramatically suppress superconductivity by pair breaking in the case of an anisotropic gap in a d-wave superconductor. Moreover, experiments on cuprates reveal [16] that a spinless impurity (Zn, Li, etc.) introduced into a HTSC host produces a large and spatially extended alternating magnetic polarization in its vicinity. Based on NMR and muon spin rotation (μSR) spectra, it has been demonstrated that this impurity-induced magnetization on the nearest-neighbor Cu atoms in cuprates is associated with a dynamic moment [16].

In the case of RB_{12}, the replacement of nonmagnetic ions of Zr by Lu produces an about 15 times' reduction of the superconducting transition temperature ($T_c \approx 0.4$ K for LuB_{12} [4,9,17]), and the origin of this large T_c suppression for these two compounds with similar conduction bands and crystalline structures is not yet clarified. Indeed, inelastic neutron scattering studies of the phonon spectra in LuB_{12} and ZrB_{12} [5] have detected noticeable, but not dramatic, changes in the position of an almost dispersionless quasilocal mode (15 and 17.5 meV, correspondingly), which was proposed to be responsible for Cooper pairing. Only a moderate difference in the electronic density of states of these two compounds can be caused by filling the wide enough conduction band ($\sim$1.6–2 eV) when Lu^{3+} ions are replaced by Zr^{4+} ions in the RB_{12} unit cell, resulting in an elevation of the Fermi level E_F of ZrB_{12} in comparison with LuB_{12} by about 0.3–0.4 eV (see Refs. [12,18] for details).

Here, we probed the evolution of the superconducting transition temperature T_c and the normal state parameters for substitutional solid solutions $Lu_xZr_{1-x}B_{12}$ using resistivity, heat capacity, and both dynamic and static magnetization measurements. It will be shown that the nonmagnetic Lu impurity substitution (having a $4f^{14}$ configuration) produces a strong static spin polarization in the vicinity of lutetium ions. Simultaneously with the emergence of static magnetic moments with a value of about $6\mu_B$ per Lu^{3+} ion ($^1S_0$ ground state), the obtained experimental results exhibit a strong suppression of superconductivity in $Lu_xZr_{1-x}B_{12}$.

*nes@lt.gpi.ru

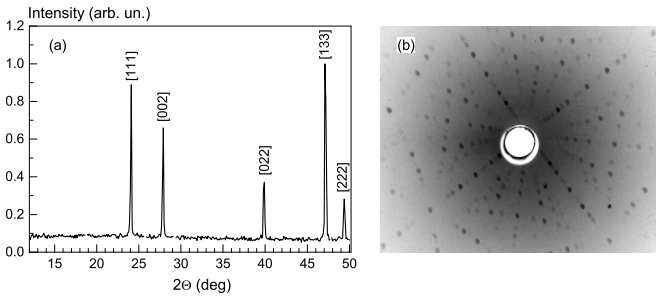

FIG. 1. (a) X-ray diffraction (from the crushed single crystal) and (b) Laue pattern of the $Lu_{0.074\pm0.001}Zr_{0.926\pm0.001}B_{12}$ single crystal (real composition) received from CoK_α radiation with a Fe filter. The crystal was grown using a [100]-oriented seed. The deviation between the growth and [100] direction is about 3°.

II. EXPERIMENTAL DETAILS

Studies of the resistivity, transverse magnetoresistance and Hall effect, heat capacity, magnetization, and electron spin resonance (ESR) of high-quality single crystals of $Lu_xZr_{1-x}B_{12}$ solid solutions with $x < 8\%$ were carried out at temperatures in the range 1.8–300 K, in magnetic fields of up to 90 kOe ($\mathbf{H}\|\langle001\rangle$). A standard dc five-probe technique was applied for resistivity and Hall effect investigations with the orientation of measuring current $\mathbf{I}\|\langle110\rangle$. The magnetization and heat capacity were measured using a Quantum Design physical properties measurement system (PPMS-9). High-frequency electron spin resonance (ESR) studies of the solid solution with $x = 7.4\%$ were made using a specially constructed spectrometer with a cylindrical cavity, operating at the transverse electric TE_{011} mode and with a quality factor $Q \sim 10^4$. Further details about the installation and measurement technique may be found elsewhere [19].

The single crystals of $Lu_xZr_{1-x}B_{12}$ were grown by vertical crucible-free inductive floating zone melting in an inert gas atmosphere. To verify both the quality of the samples and the Lu content, x-ray diffraction, Laue backscattering patterns (see Fig. 1, for example), and microanalysis techniques were used. For all $Lu_xZr_{1-x}B_{12}$ single crystals the Lu/Zr ratio was estimated using a scanning electron microscope equipped with an energy dispersion microprobe system (JEOL JXA-8200 EPMA; electron probe spot 1 μm^2). The measurements were carried out at several points of the lateral cross section (periphery $r = 1$, middle $r = 1/2$, center $r = 0$) on both sides of the single crystal rods. Individual binary borides (ZrB_2, ZrB_{12}, ZrB_{51}, and LuB_{12}) were used as reference samples. The accuracy of the microprobe analysis according to the registration certificate was several hundred ppm. The results of the analysis have shown that the single crystal real compositions differ from its initial nominal ones and vary slightly along the crystal axis, showing no dispersion in the lateral cross section.

III. RESULTS AND DISCUSSION

Temperature dependences of resistivity ρ [Fig. 2(a)], magnetization M [Fig. 2(b)], and heat capacity C [Fig. 2(c)] show superconducting phase transitions with T_c in the range 4.5–6 K for $Lu_xZr_{1-x}B_{12}$ ($x < 8\%$) solid solutions. The resistivity

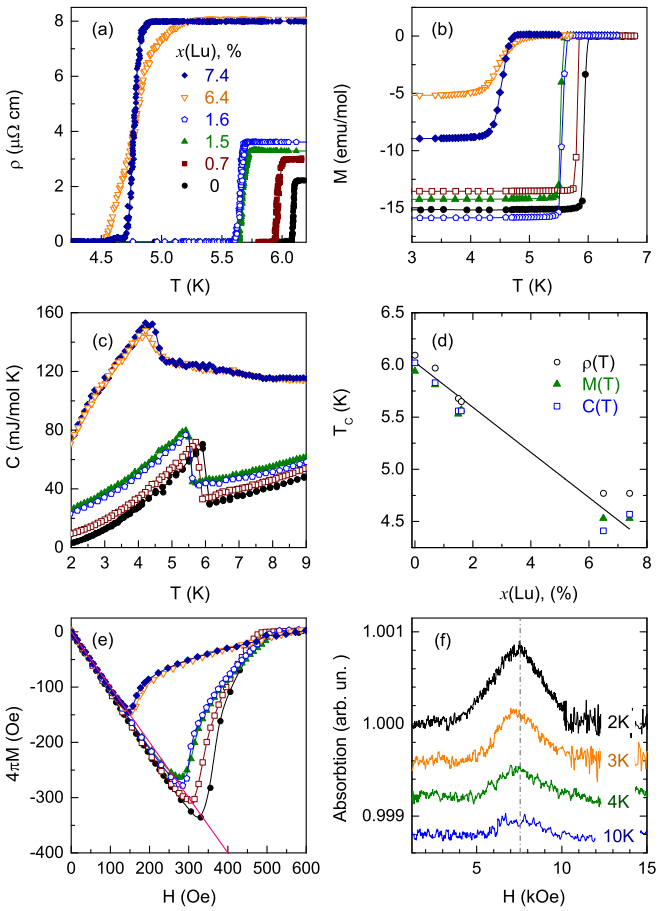

FIG. 2. Temperature dependences of (a) resistivity, (b) zero-field-cooled magnetization at $H = 3$–20 Oe, (c) specific heat in the vicinity of T_c, (d) suppression of superconductivity $T_c(x)$, and (e) the Meissner effect $M(H, T_0 = 2\ \mathrm{K})$ in $Lu_xZr_{1-x}B_{12}$. In (e), a slight increase of magnetization above the linear $M(H)$ dependence at $H > 100$ Oe is caused by a small tilt of the crystal in comparison with the applied magnetic field **H**. (f) ESR spectra measured at $f = 60$ GHz for a $Lu_{0.074}Zr_{0.926}B_{12}$ single crystal.

$\rho(T)$ drop to zero below T_c is accompanied both by the appearance of a Meissner state diamagnetic response on $M(T)$ and $M(H, T_0 = 2\ \mathrm{K})$ [Fig. 2(e)] curves and the stepwise changes in the specific heat $C(T)$ [see Figs. 2(c), 3(a), and 3(b), $H = 0$ curves]. With the increase of lutetium content both the residual resistivity and the normal state specific heat rise dramatically [by a factor of 4; see Figs. 2(a), and 3(a), and 3(b)], and the latter one demonstrates a combination of superconducting steplike and Schottky-type anomalies [see, e.g., Fig. 3(b), $H = 0$ curve for $x = 7.4\%$). It is worth noting that the Schottky-type anomaly for $Lu_{0.074}Zr_{0.926}B_{12}$ [Fig. 3(b), $H = 0$] is very similar to the one observed previously for LuB_{12} [9,20,21], and it may be interpreted in terms of the formation of double-well potentials in the disordered RB_{12} matrix of these cage-glass compounds. Comprehensive investigations of high-quality single crystals of LuB_{12} with various boron isotope compositions recently allowed one to find a new disordered cage-glass phase at liquid nitrogen temperatures [9,20]. It was shown [9,20–22] that the combination of loosely bound states of rare-earth/transition-metal ions in the rigid boron sublattice

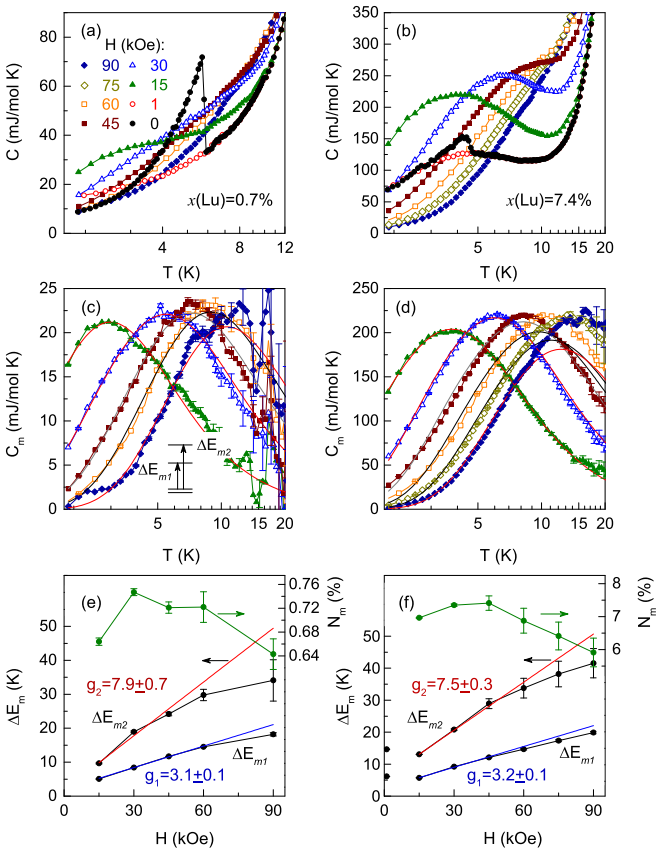

FIG. 3. Temperature dependences of specific heat for $Lu_xZr_{1-x}B_{12}$ with (a) $x = 0.7\%$ and (b) $x = 7.4\%$ in magnetic fields up to 90 kOe. (c) and (d) demonstrate the magnetic component C_m of heat capacity extracted for Lu content $x = 0.7\%$ and 7.4%, correspondingly. The fitting of $C_m(T, H_0)$ by Eq. (1) [see scheme in (c)] is shown by solid lines. The splitting energies $\Delta E_{m1}(H)$, $\Delta E_{m2}(H)$, and concentrations $N_m(H)$ are shown for $Lu_xZr_{1-x}B_{12}$ with $x = 0.7\%$ and 7.4% in (e) and (f), correspondingly.

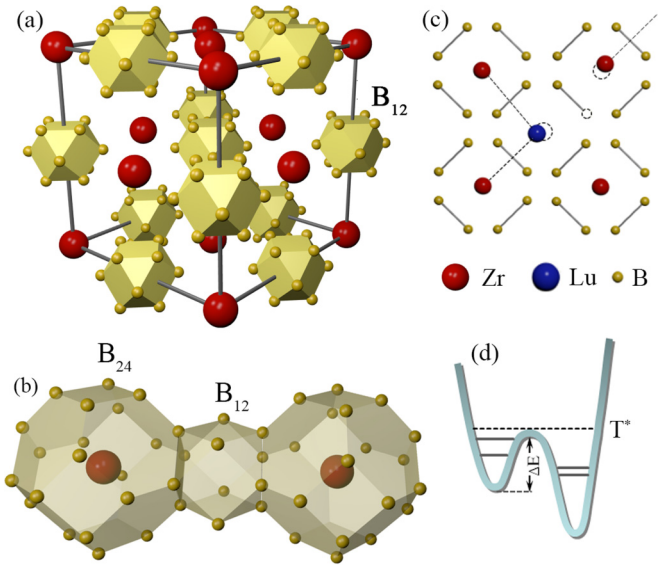

FIG. 4. (a) Crystal structure of $Lu_xZr_{1-x}B_{12}$ compounds. The NaCl-type unit cell is built from $R^{3+}(R^{4+})$ ions and B_{12} cubo-octahedrons. (b) The first coordination sphere of the R ion is arranged as a truncated octahedron B_{24}. For clarity, B_{12} and B_{24} clusters are shown only along the [100] direction of the lattice. The arrangement of R and B atoms along the [110] direction and in the (100) cross section is presented in (c). A lattice defect (boron vacancy) is shown by a small open circle (c). Broken R-B bonds in the vicinity of the boron vacancy cause displacements of the nearest R ions—they are pushed away from the defect by about 0.4 Å [23], forming a double-well potential (d) with a barrier of $\Delta E \sim T^*$ [9,20].

of RB_{12} compounds, together with randomly arranged boron vacancies (with a concentration of ~1%–3%) leads to a development of lattice instability at intermediate temperatures. As a result, in the range $T < T^* \sim 60$–80 K, metallic R^{3+} (R^{4+}) ions become frozen in randomly distributed off-centered positions inside truncated B_{24} octahedrons [Figs. 4(a)–4(d)]. Both the boson peak in low-frequency Raman spectra and the Schottky-type anomalies in the heat capacity produced by double-well potentials and two-level systems in the disordered RB_{12} matrix have been observed in studies of dodecaborides in the cage-glass state [9,20,21]. The cage-glass transition at $T^* \sim 60$ K was detected in Lu^NB_{12} crystals with various boron isotopes ($N = 10$, 11, and *natural*) in Hall effect studies [22]. The displacement of rare-earth ions from the central positions in B_{24} cubo-octahedrons was estimated from extended x-ray absorption fine structure (EXAFS) measurements to be about 0.4 Å [23]. Similar investigations of the Hall coefficient $R_H(T)$ have been undertaken here for $Lu_{0.015}Zr_{0.985}B_{12}$ and ZrB_{12}. The data of Fig. 5 demonstrate strong changes of $R_H(T)$ in the vicinity of the cage-glass temperature $T^* \sim 80$ K. We estimated also the Hall mobility $\mu_H(T) = R_H(T)/\rho(T)$ in the studied compounds (see the inset in Fig. 5). Although $\mu_H(T)$ is small enough (the inset in Fig. 5, $\mu_H < 100$ cm^2/V s), both their temperature dependence and charge carrier concentration values $n_e = 2.3$–2.6×10^{22} cm^{-3} derived from the $R_H(T)$ data of Figs. 5(a) and 5(b) are typical for compounds with a metallic conduction.

Then, coming back to the discussion of the Schottky-type anomaly and the about fourfold increase of $C(T, H = 0)$ at low temperatures [Figs. 3(a) and 3(b)], it is worth noting that evidently these features cannot be considered as caused by renormalization of the Sommerfeld coefficient of the electronic heat capacity. It will be shown below that the $C(T)$ maximum increases essentially in the magnetic field and that this increase should be attributed to an additional, magnetic component of heat capacity.

The $T_c(x)$ dependence for $Lu_xZr_{1-x}B_{12}$ solid solutions is summarized in Fig. 2(d). T_c was defined as a midpoint of resistivity (magnetization) changes within the transition to the superconducting state. It should be stressed that the suppression of superconductivity by Lu substitution is unusually strong (~0.21 K/at. % Lu), when supposing the doping of an s-wave superconductor by nonmagnetic impurities. On the other hand, only a value of $\Delta T_c/\Delta x \sim 0.06$ K/at. % Ta was detected in Ref. [24] for Nb-Ta alloys.

In an external magnetic field the amplitude of the low-temperature Schottky-type anomaly increases essentially and $C(T)$ maximum moves to higher temperatures [for example, Figs. 3(a) and 3(b) show the data for $x = 0.7\%$ and 7.4%, correspondingly]. Evidently, the Zeeman component is a

magnetic contribution to heat capacity and it may be separated from vibrational and electron heat capacity terms following the approach developed in Refs. [20,21]. In particular, we take here the specific heat $C(T, H = 0)$ dependence of ZrB_{12} as a reference curve with a correction of the Einstein term by changing Θ_E from $\Theta_E(ZrB_{12}) \approx 200$ K to $\Theta_E(LuB_{12}) \approx 162$ K, in accordance with a Lu concentration increase in $Lu_xZr_{1-x}B_{12}$ solid solutions [21]. The resulting $C_m(T, H_0)$ dependences for these two Lu contents are presented in Figs. 3(c) and 3(d), together with their approximation [see the solid lines in Figs. 3(c) and 3(d)] based on a four-level Schottky relation with a doublet ground state [see the scheme in Fig. 3(c)],

$$C_m = N_m R\beta^2 \frac{2\Delta E_{m1}^2\, e^{-\beta\Delta E_{m1}} + 2\Delta E_{m2}^2\, e^{-\beta\Delta E_{m2}} + (\Delta E_{m1} - \Delta E_{m2})^2\, e^{-\beta(\Delta E_{m1}+\Delta E_{m2})}}{(g_0 + e^{-\beta\Delta E_{m1}} + e^{-\beta\Delta E_{m2}})^2},$$
$$\beta = 1/T \quad (k_B = 1), \tag{1}$$

where R and k_B denote the universal gas and Boltzmann constants, correspondingly, $g_0 = 2$ is the degeneracy of the ground state, and N_m is the concentration of magnetic sites. It is worth noting that these $C_m(T, H_0)$ anomalies are broad enough to be fitted by the simplest Schottky relation for a single two-level system (TLS). So, instead of two different TLS_1 and TLS_2, we have used here a four-level scheme [Fig. 3(c)] both to reduce the number of fitting parameters and to choose the correct concentration N_m of magnetic sites. Both splitting energies $\Delta E_{m1}(H)$ and $\Delta E_{m2}(H)$ and the concentration of magnetic Schottky sites $N_m(H)$ as deduced from the approximation (1) are shown in Figs. 3(e) and 3(f).

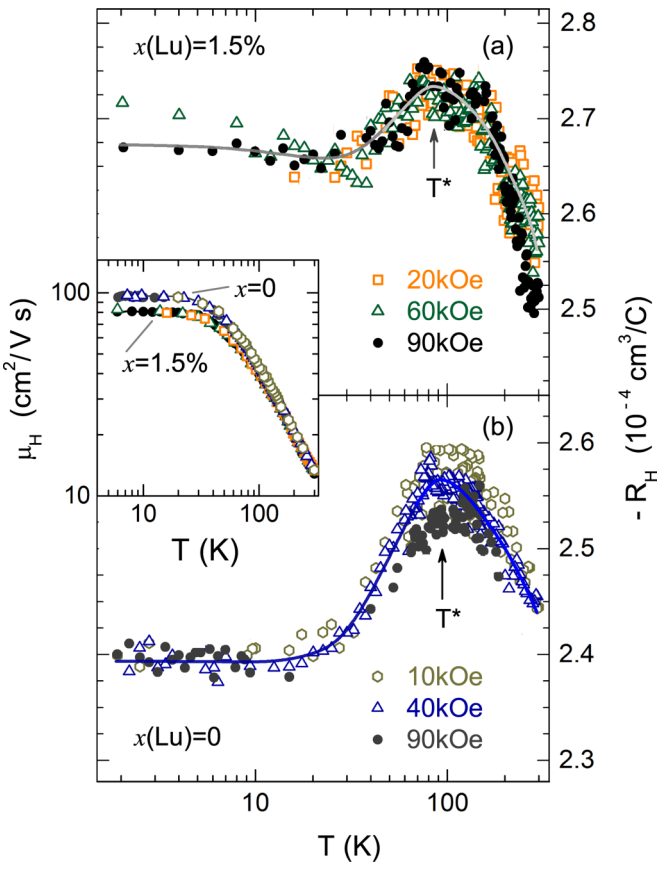

FIG. 5. Temperature dependences of Hall coefficient $R_H(T)$ for $Lu_xZr_{1-x}B_{12}$ with (a) $x = 1.5\%$ and (b) $x = 0$ in magnetic fields up to 90 kOe. The inset shows the behavior of Hall mobility $\mu_H(T) = R_H(T)/\rho(T)$ vs temperature.

The slope of the straight lines in Figs. 3(e) and 3(f) (in the range $H < 40$ kOe) allows one to determine from the relation $\Delta E_{mi} = \mu_B g_i H/k_B$ the g factors $g_1 \sim 3.2$ and $g_2 \sim 7.8$ for both studied crystals (see Table I). Moreover, the concentration of N_m is found to be equal within experimental accuracy to lutetium content x in $Lu_xZr_{1-x}B_{12}$ solid solutions. From these results it may be certainly concluded that magnetic sites are created by Lu impurities (Table I).

The magnetic response in the normal state of $Lu_xZr_{1-x}B_{12}$ superconductors was investigated by magnetization $M(H,T)$ studies. Figures 6(a) and 6(b) demonstrate the temperature dependences $M(H_0,T)$ recorded at $H_0 = 2$ kOe and the magnetization versus magnetic field curves $M(H,T_0)$ measured at $T_0 = 2$ K, correspondingly. It can be seen from Fig. 6(a) that a small ($\sim 4 \times 10^{-4}\mu_B$/Zr) and about temperature-independent Pauli-like paramagnetic response, which is typical for ZrB_{12}, changes into a Curie-Weiss-type magnetic signal originating from magnetic moments induced by the Lu substitution. Fitting the temperature dependences by the Curie-Weiss relation

$$M = \chi_0 H + N_m \mu_{\text{eff}}^2 H/[3k_B(T - \Theta)], \tag{2}$$

where χ_0 is the temperature-independent susceptibility, μ_{eff} the effective magnetic moment in Bohr magnetons μ_B, and Θ is the Curie-Weiss temperature [see the solid lines in Fig. 6(a)] allows one to determine the Curie constant and subsequently to estimate the effective magnetic moment $\mu_{\text{eff}} \sim 5.7$–$6.6\mu_B$ per Lu ion (see also Table I). These values are about twice higher compared with the saturated moments $\mu_{\text{sat}} \sim 3$–$4\mu_B$ per Lu ion obtained from the analysis of magnetization versus magnetic field dependences [Fig. 6(b)]. Moreover, in the regime of an isolated magnetic impurity for $x = 0.7\%$, the magnetization may be described with a good accuracy by the Brillouin-type dependence

$$M = N_m g \mu_B J B_J(g\mu_B J H/k_B T) \tag{3}$$

(where B_J is the Brillouin function, and $J = 3/2$ is the angular momentum of the quartet state), with $N_m \approx 0.54x$, $g \approx 3.5$. Because of the equidistant location of four $(2J + 1)$ singlet states in the Brillouin-type approximation, we obtained a twice reduced estimation for the concentration of magnetic sites in comparison with N_m for the doublet-singlet-singlet configuration [see Fig. 3(c)]. Simultaneously, Curie-Weiss-type fitting provides an appropriate value for the g factor $g \approx 6$ of these magnetic states in $Lu_xZr_{1-x}B_{12}$ superconductors. Moreover, Fig. 2(f) presents also our latest results of an ESR study performed on a $Lu_{0.074}Zr_{0.926}B_{12}$ crystal at temperatures

TABLE I. The parameters of heat capacity and magnetization analysis performed for $Lu_xZr_{1-x}B_{12}$.

	$C(T,H)$			$M(T,H)$		
x (%)	g_1	g_2	N_m (%)	$\mu_{\rm eff}$ (μ_B/Lu)	$\mu_{\rm sat}$ (μ_B/Lu)	χ_0 ($10^{-5}\mu_B$/kOe)
0.7	3.1 ± 0.1	7.9 ± 0.7	0.7 ± 0.04	5.7	2.9	2.3
1.5	3.3 ± 0.3	7.8 ± 0.2	2.1 ± 0.1	6.6	4.3	-4.6
1.6	3.0 ± 0.1	7.6 ± 0.7	1.8 ± 0.2	6.3	3.7	11.2
6.5	3.5 ± 0.2	6.8 ± 0.1	7.2 ± 0.3	6.1	3.4	11.4
7.4	3.2 ± 0.1	7.5 ± 0.3	6.8 ± 0.6	5.7	3.0	3.3

in the range 1.8–10 K. The observed single ESR line allowed us to estimate the g factor as $g = 5.7 \pm 0.1$ ($H_{\rm res} \approx 7.5$ kOe) for these oscillating magnetic moments. The detected linewidth $\Delta H \approx 2.7$ kOe corresponds to a spin relaxation time $\tau \approx 2.9 \times 10^{-10}$ s. It is worth noting that a similar magnetic component in heat capacity has been observed in the nonmagnetic Heusler-type compound Fe_2VAl [25], indicating the presence of Schottky anomalies arising from magnetic clusters having a moment of $3.7\mu_B$ and $J = 3/2$.

Magnetoresistance $\Delta\rho/\rho$ experiments were performed also in the normal state ($H > 0.8$ kOe) to characterize the magnetic moments in these $Lu_xZr_{1-x}B_{12}$ compounds with metallic conduction. According to Yosida calculations carried out within the framework of the *s-d* exchange model, an appearance of negative magnetoresistance (nMR) is expected in the regime of charge carrier scattering on localized magnetic moments [26]. The field dependence of nMR is controlled by local magnetization $M_{\rm loc}$ through the relation

$$-\Delta\rho/\rho \sim M_{\rm loc}^2. \quad (4)$$

The nMR effect may be considered as an independent argument in favor of the formation of local moments in a metallic matrix. Figure 7 shows the results of magnetoresistance measurements on $Lu_xZr_{1-x}B_{12}$. In the normal state of ZrB_{12} the main contribution to $\Delta\rho/\rho(H,T_0)$ is positive and it can be described with good accuracy by the well-known relation $\Delta\rho/\rho \sim \mu_{\rm D}^2 H^2$, where $\mu_{\rm D}$ is the carriers' drift mobility. Both the substitutional disorder and the cage-glass effect in $Lu_xZr_{1-x}B_{12}$ decrease dramatically both the mobility and amplitude of the positive component when the Lu concentration increases [Fig. 7(a)]. For $x \geqslant 1.5\%$ the appearance of a nMR contribution to $\Delta\rho/\rho$ becomes evident, and for $x \sim 7\%$ the negative term in the applied magnetic fields [Fig. 7(a)] prevails. Figure 7(b) presents a set of magnetic field dependences $\Delta\rho/\rho(H,T_0)$ obtained for $x = 1.5\%$ at temperatures between 1.8 and 8 K. When the temperature decreases in the range 1.85–4 K, a crossover from positive magnetoresistance to a combination of positive and negative components is observed, and similar to the approach developed in Ref. [27], these data may be approximated very well by the relation

$$\Delta\rho/\rho = \mu_{\rm D}^2 H^2 - [Ag\mu_B J B_J(g\mu_B JH/k_BT)]^2, \quad (5)$$

where $A \sim N_m$ is the normalized concentration of these magnetic moments. Fitting data by relation (5) [see the solid lines in Fig. 7(b)] allows one to estimate the g factor $g \approx 3.5$ for the angular momentum $J = 3/2$. The obtained values are in accordance with those deduced above from the analysis of heat capacity and magnetization (Table I). Additionally, we have evaluated the behavior of coefficients $A(T)$ and $\mu_{\rm D}(T)$ in (5) [see Figs. 7(c) and 7(d), correspondingly]. As can be seen from Fig. 7(c), the scattering of charge carriers on localized moments in the vicinity of impurity sites appears below 8 K and it increases drastically with decreasing temperature. On the contrary, the $\mu_{\rm D}(T)$ dependence demonstrates only a moderate elevation (<4%) with a temperature decrease in the range 2–8 K [Fig. 7(d)], in accordance with $\mu_H(T)$ behavior (the inset in Fig. 5). Thus, these positive and negative components of magnetoresistance become comparable at helium temperatures and in magnetic fields below 40 kOe.

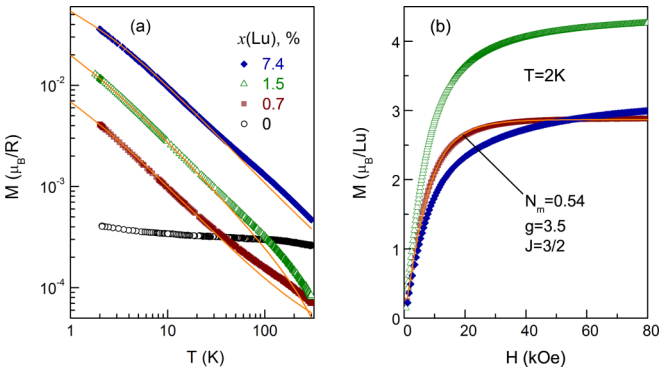

FIG. 6. Dependences of magnetization vs temperature at $H_0 = 2$ kOe (a) and vs magnetic field at $T_0 = 2$ K (b) for $Lu_xZr_{1-x}B_{12}$. Approximations by the (a) Curie-Weiss relation [Eq. (2)] and by the (b) Brillouin dependence [Eq. (3)] are shown by solid lines.

When discussing the possible scenario of the formation of spin-polarized nanodomains in $Lu_xZr_{1-x}B_{12}$ substitutional solid solutions, it is worth noting the mechanism of spin-polaron formation proposed for magnetic rare-earth higher borides with a cage-glass structure. It was suggested in Ref. [28] that fast quantum oscillations (tunneling) of magnetic rare-earth ions in a double-well potential lead to spin polarization of $5d$ states of the conduction band, and this effect appears to be very sensitive to an external magnetic field. When taking into account that in LuB_{12} the $4f$ band is located well below (~5 eV) the Fermi level [18,29], there is a strong presumption against the $4f$ nature of these moments in the ZrB_{12} matrix. Among the possible scenarios of the formation of magnetic moments in the vicinity of Lu ions, one can propose the induced spin polarization of $4d$(Zr) or $5d$(Lu) states. In this connection we can mention also the analogy with another Zr-based metallic compound, $ZrZn_2$, in which a coexistence of spin-triplet superconductivity with

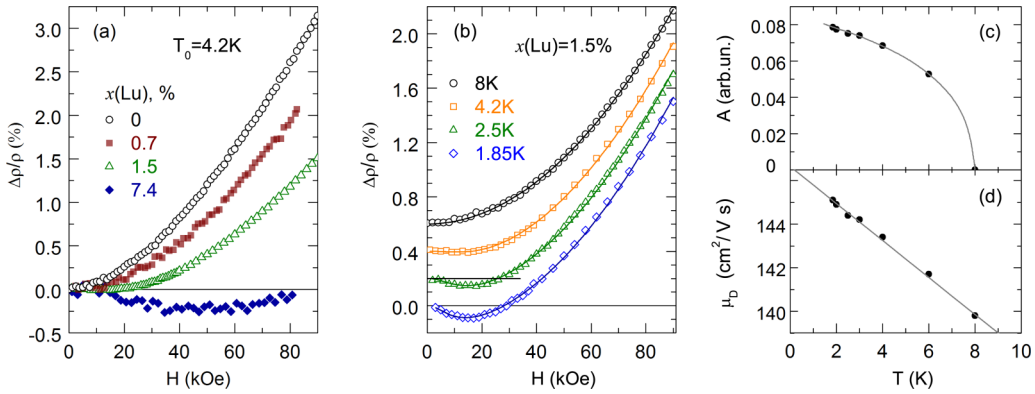

FIG. 7. Magnetic field dependences of normal state magnetoresistance $\Delta\rho/\rho(H,T_0) = [\rho(H) - \rho(0.8\ \text{kOe})]/\rho(0.8\ \text{kOe})$ (a) for $Lu_xZr_{1-x}B_{12}$ with various Lu content at $T_0 = 4.2$ K, and (b) for $x = 1.5\%$ at temperatures in the range 1.85–8 K. Approximations in the framework of Eq. (5) are shown by solid lines in (b); curves are shifted by 0.2% for convenience. (c) and (d) demonstrate temperature dependences of $A(T)$ and $\mu_D(T)$ parameters in Eq. (5) extracted for $x = 1.5\%$.

weak itinerant ferromagnetism was suggested [30]. Thus, both Lu-Zr dimer formation and strong distortions of the crystalline and electronic structure in the vicinity of Lu^{3+} impurities, which are caused by nonisovalent Zr^{4+} to Lu^{3+} substitution, can be considered as mechanisms responsible for the creation of double-well potentials, and subsequently for the formation of magnetic moments on the $4d$ ($5d$) states of Zr (Lu) ions. For any of these two scenarios the size of the induced magnetic nanodomains may be estimated as comparable with the $R - R$ distance which is about 5 Å in the lattice of $Lu_xZr_{1-x}B_{12}$ dodecaborides. It should be also stressed that the origin of these many-body states described by the four-level schema with $J = 3/2$ both in Ref. [25] and here is not yet fully clarified. So, the elucidation of the anisotropy produced by these magnetic clusters needs to be further elaborated. Turning to the analogy with nonmagnetic impurity-induced *dynamic* moments in HTSC cuprates, it should be stressed here that the localized moments found in the present study of $Lu_xZr_{1-x}B_{12}$ are *static* and that a strong enhancement of spin polarization (exhibiting a saturation above 40 kOe) is induced by an external magnetic field. Thus, the pair breaking produced by nonmagnetic Lu^{3+} ions incorporated in ZrB_{12} is quite similar to the effect of magnetic impurity doping in conventional superconductors.

IV. CONCLUSIONS

We have observed the formation of static nanosized magnetic moments with $\mu_{\text{eff}} \approx 6\mu_B$ per Lu^{3+} ion in the vicinity of nonmagnetic lutetium impurities in the nonmagnetic Zr-rich matrix of $Lu_xZr_{1-x}B_{12}$ dodecaborides at low temperatures. According to our opinion, the strong suppression of superconductivity in $Lu_xZr_{1-x}B_{12}$ compounds can be attributed to pair breaking arising in the vicinity of these nanosized magnetic domains. However, for the correct decision both about the nature of magnetic moments in the ZrB_{12} matrix and about the mechanism of superconductivity in $Lu_xZr_{1-x}B_{12}$ with high Lu contents, it will be necessary to investigate new crystals with x in the ranges 2%–6% and $x > 7\%$ of Lu.

ACKNOWLEDGMENTS

We would like to thank A. V. Kuznetsov, G. E. Grechnev, A. V. Semeno, P. Samuely, and S. Gabani for helpful discussions. The study was supported by RFBR Project No. 15-02-02553a, Young Scientists Grant of the RF President No. MK-6427.2014.2. The measurements were carried out in the Shared Facility Centre of P. N. Lebedev Physical Institute of RAS. K.F. acknowledges partial support by Slovak agencies VEGA (2/0106/13) and APVV (14-0605).

[1] J. Nagamatsu, N. Nakagawa, T. Muranaka, Y. Zenitani, and J. Akimitsu, Nature (London) **410**, 63 (2001).
[2] R. Lortz, Y. Wang, S. Abe, C. Meingast, Yu. B. Paderno, V. Filippov, and A. Junod, Phys. Rev. B **72**, 024547 (2005).
[3] Y. Wang, R. Lortz, Yu. B. Paderno, V. Filippov, S. Abe, U. Tutsch, and A. Junod, Phys. Rev. B **72**, 024548 (2005).
[4] J. Teyssier, R. Lortz, A. Petrovic, D. van der Marel, V. Filippov, and N. Shitsevalova, Phys. Rev. B **78**, 134504 (2008).
[5] A. V. Rybina, K. S. Nemkovski, P. A. Alekseev, J.-M. Mignot, E. S. Clementyev, M. Johnson, L. Capogna, A. V. Dukhnenko, A. B. Lyashenko, and V. B. Filippov, Phys. Rev. B **82**, 024302 (2010).
[6] M. I. Tsindlekht, G. I. Leviev, I. Asulin, A. Sharoni, O. Millo, I. Felner, Yu. B. Paderno, V. B. Filippov, and M. A. Belogolovskii, Phys. Rev. B **69**, 212508 (2004).
[7] G. I. Leviev, V. M. Genkin, M. I. Tsindlekht, I. Felner, Yu. B. Paderno, and V. B. Filippov, Phys. Rev. B **71**, 064506 (2005).
[8] D. Daghero, R. S. Gonnelli, G. A. Ummarino, A. Calzolari, V. Dellarocca, V. A. Stepanov, V. B. Filippov, and Yu. B. Paderno, Supercond. Sci. Technol. **17**, S250 (2004).
[9] N. Sluchanko, S. Gavrilkin, K. Mitsen, A. Kuznetsov, I. Sannikov, V. Glushkov, S. Demishev, A. Azarevich, A. Bogach, A. Lyashenko, A. Dukhnenko, V. Filipov, S. Gabáni, K. Flachbart, J. Vanacken, G. Zhang, and V. Moshchalkov, J. Supercond. Novel Magn. **26**, 1663 (2013).
[10] J. Auer and H. Ullmaier, Phys. Rev. B **7**, 136 (1973).

[11] V. A. Gasparov, N. S. Sidorov, and I. I. Zver'kova, Phys. Rev. B **73**, 094510 (2006).
[12] S. Thakur, D. Biswas, N. Sahadev, P. K. Biswas, G. Balakrishnan, and K. Maiti, Sci. Rep. **3**, 03342 (2013).
[13] P. W. Anderson, Phys. Rev. Lett. **3**, 325 (1959).
[14] A. A. Abrikosov and L. P. Gor'kov, Zh. Exp. Theor. Phys. **39**, 1781 (1960) [Sov. Phys. JETP **12**, 1243 (1961)].
[15] A. V. Balatsky, I. Vekhter, and J. X. Zhu, Rev. Mod. Phys. **78**, 373 (2006).
[16] H. Alloul, J. Bobroff, M. Gabay, and P. J. Hirschfeld, Rev. Mod. Phys. **81**, 45 (2009).
[17] K. Flachbart, S. Gabáni, K. Gloos, M. Meissner, M. Opel, Yu. Paderno, V. Pavlík, P. Samuely, E. Schuberth, N. Shitsevalova, K. Siemensmeyer, and P. Szabó, J. Low Temp. Phys. **140**, 339 (2005).
[18] B. Jäger, S. Paluch, O. J. Żogał, W. Wolf, P. Herzig, V. B. Filippov, N. Yu. Shitsevalova, and Yu. B. Paderno, J. Phys.: Condens. Matter **18**, 2525 (2006).
[19] A. N. Samarin, A. V. Semeno, M. I. Gilmanov, V. V. Glushkov, I. I. Lobanova, N. A. Samarin, N. E. Sluchanko, I. I. Sannikov, N. M. Chubova, V. A. Dyadkin, S. V. Grigoriev, and S. V. Demishev, Phys. Procedia **71**, 337 (2015).
[20] N. E. Sluchanko, A. N. Azarevich, A. V. Bogach, I. I. Vlasov, V. V. Glushkov, S. V. Demishev, A. A. Maksimov, I. I. Tartakovskii, E. V. Filatov, K. Flachbart, S. Gabáni, V. B. Filippov, N. Yu. Shitsevalova, and V. V. Moshchalkov, J. Exp. Theor. Phys. **113**, 468 (2011).
[21] N. E. Sluchanko, A. N. Azarevich, S. Yu. Gavrilkin, V. V. Glushkov, S. V. Demishev, N. Yu. Shitsevalova, and V. B. Filippov, JETP Lett. **98**, 578 (2013).
[22] N. E. Sluchanko, A. N. Azarevich, A. V. Bogach, V. V. Glushkov, S. V. Demishev, A. V. Kuznetsov, K. S. Lyubshov, V. B. Filippov, and N. Yu. Shitsevalova, J. Exp. Theor. Phys. **111**, 279 (2010).
[23] A. P. Menushenkov, A. A. Yaroslavtsev, I. A. Zaluzhnyy, A. V. Kuznetsov, R. V. Chernikov, N. Yu. Shitsevalova, and V. B. Filippov, JETP Lett. **98**, 165 (2013).
[24] T. McConville and B. Serin, Phys. Rev. **140**, A1169 (1965).
[25] C. S. Lue, J. H. Ross, Jr., C. F. Chang, and H. D. Yang, Phys. Rev. B **60**, R13941(R) (1999).
[26] K. Yosida, Phys. Rev. **107**, 396 (1957).
[27] N. E. Sluchanko, A. L. Khoroshilov, M. A. Anisimov, A. N. Azarevich, A. V. Bogach, V. V. Glushkov, S. V. Demishev, V. N. Krasnorussky, N. A. Samarin, N. Yu. Shitsevalova, V. B. Filippov, A. V. Levchenko, G. Pristáš, S. Gabáni, and K. Flachbart, Phys. Rev. B **91**, 235104 (2015).
[28] N. E. Sluchanko, Low Temp. Phys. **41**, 544 (2015).
[29] G. E. Grechnev, A. E. Baranovskiy, V. D. Fil, T. V. Ignatova, I. G. Kolobov, A. V. Logosha, N. Yu. Shitsevalova, V. B. Filippov, and O. Eriksson, Low Temp. Phys. **34**, 921 (2008).
[30] C. Pfleiderer, M. Uhlarz, S. M. Hayden, R. Vollmer, H. V. Löhneysen, N. R. Bernhoeft, and G. G. Lonzarich, Nature (London) **412**, 58 (2001).